HHS Public Access

Author manuscript

Cell Stem Cell. Author manuscript; available in PMC 2015 April 08.

Published in final edited form as:

Cell Stem Cell. 2015 January 8; 16(1): 39–50. doi:10.1016/j.stem.2014.10.019.

Inhibition of Pluripotency Networks by the Rb Tumor Suppressor Restricts Reprogramming and Tumorigenesis

Michael S. Kareta[1,2,3,6], **Laura L. Gorges**[1,2], **Sana Hafeez**[3,6], **Bérénice A. Benayoun**[2,7], **Samuele Marro**[3,6], **Anne-Flore Zmoos**[1,2], **Matthew J. Cecchini**[8], **Damek Spacek**[1,2], **Luis F.Z. Batista**[4,5,6], **Megan O'Brien**[1,2], **Yi-Han Ng**[3,6], **Cheen Euong Ang**[3,6], **Dedeepya Vaka**[1,2], **Steven E. Artandi**[4,5,6], **Frederick A. Dick**[8], **Anne Brunet**[2,7], **Julien Sage**[1,2,9,*], and **Marius Wernig**[3,6,9,*]

[1]Department of Pediatrics, Stanford University, Stanford, CA 94305, USA

[2]Department of Genetics, Stanford University, Stanford, CA 94305, USA

[3]Department of Pathology, Stanford University, Stanford, CA 94305, USA

[4]Department of Medicine, Stanford University, Stanford, CA 94305, USA

[5]Department of Biochemistry, Stanford University, Stanford, CA 94305, USA

[6]Stanford Institute for Stem Cell Biology and Regenerative Medicine, Stanford University, Stanford, CA 94305, USA

[7]Paul F. Glenn Laboratories for the Biology of Aging, Stanford University, Stanford, CA 94305, USA

[8]London Regional Cancer Program, Children's Research Institute, Western University, London, ON N6A 4L6, Canada

SUMMARY

Mutations in the retinoblastoma tumor suppressor gene *Rb* are involved in many forms of human cancer. In this study, we investigated the early consequences of inactivating Rb in the context of cellular reprogramming. We found that Rb inactivation promotes the reprogramming of

*Correspondence: julsage@stanford.edu (J.S.), wernig@stanford.edu (M.W.).
[9]Co-senior author

ACCESSION NUMBERS

The data for RNA and ChIP sequencing have been deposited in NCBI's Gene Expression Omnibus and are accessible through GEO Series accession number GSE40594 (http://www.ncbi.nlm.nih.gov/geo/query/acc.cgi?acc=GSE40594).

SUPPLEMENTAL INFORMATION

Supplemental Information for this article includes six figures, five tables, and Supplemental Experimental Procedures and can be found with this article online at http://dx.doi.org/10.1016/j.stem.2014.10.019.

AUTHOR CONTRIBUTIONS

M.S.K. was responsible for the experiment design, execution, data analysis, and manuscript preparation. L.G. and L.F.Z.B. aided in the initial reprogramming assays. S.H. and M.O. aided with the efficiency assays. B.A.B. performed the broad domain analysis. S.M. performed Southern blotting. D.S. performed histone ChIP-qPCR. Y.H.N. made the chimeric mice. C.E.A. performed high-throughput imaging for cell seeding. A.-F.Z. bred the mice. M.J.C. generated the ΔG mouse line and isolated MEFs. D.V. advised on sequence analysis. S.A. advised on the human reprogramming. F.A.D. advised on Rb domain mutagenesis and manuscript review. A.B. advised on the broad domain analysis. J.S. and M.W. were equally responsible for supervision of research, data interpretation, and manuscript preparation.

differentiated cells to a pluripotent state. Unexpectedly, this effect is cell cycle independent, and instead reflects direct binding of Rb to pluripotency genes, including *Sox2* and *Oct4*, which leads to a repressed chromatin state. More broadly, this regulation of pluripotency networks and *Sox2* in particular is critical for the initiation of tumors upon loss of Rb in mice. These studies therefore identify Rb as a global transcriptional repressor of pluripotency networks, providing a molecular basis for previous reports about its involvement in cell fate pliability, and implicate misregulation of pluripotency factors such as *Sox2* in tumorigenesis related to loss of Rb function.

INTRODUCTION

The retinoblastoma gene product Rb is a potent suppressor of the tumorigenic process and is genetically or functionally inactivated in most, if not all, human cancers by direct mutation or alterations in upstream pathway members (Burkhart and Sage, 2008). Loss of Rb function has been directly implicated in initiation of cancers, including retinoblastoma, osteosarcoma, and small cell lung carcinoma in patients, as well as pituitary and thyroid tumors in mice (Chinnam and Goodrich, 2011). Rb controls multiple cellular functions, including proliferation, survival, differentiation, metabolism, and genomic stability, but how loss of Rb initiates cancer is still not completely understood (reviewed in Chinnam and Goodrich, 2011; Manning and Dyson, 2012; Nicolay and Dyson, 2013; Viatour and Sage, 2011).

Induced pluripotent stem cells (iPSCs) and embryonic stem cells (ESCs) share some similarities to cancer cells, including the capacity to bypass senescence and form tumors upon transplantation (Goding et al., 2014). Accordingly, some genes often associated with cancer, such as *Myc* (Nakagawa et al., 2008; Wernig et al., 2008), *p53* (Krizhanovsky and Lowe, 2009), and telomerase (Batista et al., 2011; Park et al., 2008), have been implicated in cellular reprogramming. Additionally, two reprogramming factors, *Oct4* and *Sox2*, can be oncogenic in some cellular contexts (Hochedlinger et al., 2005; Lu et al., 2010; Rudin et al., 2012; Sarkar and Hochedlinger, 2013).

Given previous observations that Rb could be involved in cellular dedifferentiation (Calo et al., 2010; McEvoy et al., 2011) and given the similarities between reprogramming and some aspects of tumorigenesis, we set out to identify mechanisms by which Rb suppresses dedifferentiation using iPSC reprogramming as a cellular system. We found that *Rb* regulates the reprogramming of fibroblasts to iPSCs. Surprisingly, this phenomenon is not due to changes in the cell cycle. Instead, Rb globally represses pluripotency networks in somatic cells, thereby rendering cells more amenable to reprogramming, including in the absence of exogenous *Sox2*. Importantly, pituitary hyperplasia driven by Rb loss in mice is blocked by *Sox2* deletion, expanding the functional interaction between *Rb* and *Sox2* to cancer.

RESULTS

Rb Loss Promotes Reprogramming to iPSCs

To test whether Rb regulates the reprogramming process, we infected wild-type and $Rb^{-/-}$ mouse embryonic fibroblasts (MEFs) with lentiviruses harboring the traditional four

reprogramming factors (4F), *Oct4*, *Sox2*, *Klf4*, and *c-Myc*. Based on the appearance of alkaline phosphatase $(AP)^+$ colonies, we saw more efficient reprogramming in Rb mutant MEFs than in WT cells, suggesting that loss of Rb facilitates reprogramming (Figures 1A and 1B). A similar increase in AP^+ colonies was observed with human fibroblasts expressing shRNAs to knock down human *RB* (shRB) (Figure 1A and Figure S1A available online). Because AP is not a specific marker of pluripotency, we then used *Oct4-Neo*^{R} knockin MEFs in combination with *Rb* knockdown (Figure S1B) and counted neomycin-resistant colonies. To avoid errors due to reseeding of daughter colonies, we performed a 96-well assay and quantified the wells that contained iPSC colonies rather than the number of colonies themselves. In this stringent assay, the reprogramming efficiency was increased in Rb-deficient cells to a similar degree to that reported in cells with a loss of p53 (Figures 1B and 1C) (Krizhanovsky and Lowe, 2009). Notably, Rb loss decreased the plating efficiency of MEFs (Figure S1C), illustrating our underestimation of the efficiency of reprogramming upon *Rb* loss. Reprogramming was increased by multiple hairpins against *Rb* (Figure 1B) upon acute deletion of *Rb* in *Rb*$^{lox/lox}$ conditional knockout MEFs (cKO MEFs) after adenoviral Cre (Ad-Cre) delivery (Figure 1D) and after treatment with 4-hydroxytamoxifen (4OHT) in *Rosa26*^{CreER} cKO MEFs (Figure S1D and S1E). Conversely, overexpression of *Rb* reduced the reprogramming efficiency (Figure 1E). MEFs deficient for p107 or p130, two factors closely related to Rb, showed no changes in their reprogramming efficiency (Figure 1F). Triple knockout MEFs for the entire *Rb* family (TKOs) did not reprogram to iPSCs, presumably due to an unidentified stress response that leads to increased apoptosis during reprogramming (Figure S1F).

To further determine the kinetics of reprogramming in the absence of *Rb*, we reprogrammed *Oct4-GFP* knockin MEFs after *Rb* knockdown. Colonies re-expressing endogenous *Oct4* (GFP^+) appeared significantly more quickly in cells with low *Rb* levels (Figure 1G). Utilizing SSEA1 expression as an early marker of reprogramming (Brambrink et al., 2008), we observed that *Rb* loss increases reprogramming as early as days 4 and 6 (Figure 1H, Figure S1G). To test the time requirement for the exogenous factors to trigger full reprogramming, we used *Oct4-GFP;M2rtTA* MEFs infected with a doxycycline (Dox)-inducible 4F lentiviral construct. After a total of 15 days and varying the length of Dox treatment, the number of GFP^+ iPSC colonies was counted. Decreased *Rb* levels led to a significant reduction in the time requirement for 4F expression to achieve reprogramming (Figure 1I). Together, these data demonstrate that *Rb* loss accelerates and enhances iPSC generation from fibroblasts, indicating that *Rb* normally restricts this process.

Rb Loss Does Not Accelerate the Cell Cycle during Reprogramming

One explanation for the increased reprogramming observed in *Rb*-deficient cells is a faster cell cycle, as in *p53* mutant cells (Hanna et al., 2009). We determined the doubling time of control and *Rb* knockdown MEFs in the first 10 days of the process to avoid the confounding effects of increased proliferation due to enhanced reprogramming in Rb mutant cells. Notably, no significant change in the growth rate of the 4F-infected MEFs was observed upon *Rb* knockdown (Figure 2A), as was previously observed in *Rb*-deficient MEFs (Dannenberg et al., 2000; Sage et al., 2000) (see below). Similarly, there was no change in the S phase fraction in the shRb-infected MEFs, although, at day 6 there was a

trend to a longer G2 and shorter G1 (Figures 2B and 2C, Figure S2A), possibly a consequence of increased reprogramming because a shorter G1 correlates with the acquisition of pluripotency (Conklin and Sage, 2009). Annexin V staining did not show a significant difference in apoptosis (Figure 2D, Figure S2B). To quantify proliferation specifically in reprogramming cells, we focused on $SSEA1^+$ cells and used Carboxyfluorescein diacetate succinimidyl ester (CFSE) pulse-chase staining to determine the number of cell divisions after the induction of reprogramming (Koche et al., 2011). Using an automated analysis, we confirmed that $SSEA1^+$ cells are proliferative (Figure S2C and S2D) and, importantly, we found no change in the number of doublings between control and *Rb* knockdown populations (Figure 2E). Thus, the enhanced reprogramming efficiency and kinetics observed in the absence of *Rb* cannot be simply explained by changes in cell cycle profiles.

Rb Binds to and Represses Pluripotency Genes

Next we sought to explore how the absence of the Rb protein might render MEFs more amenable to reprogramming. Because Rb is a transcriptional coregulator, we determined the consequence of *Rb* loss on gene expression. To this end, cKO MEFs were infected with Ad-Cre or Ad-GFP (Figure S3A and S3B) and infected by the 4F or an empty vector; 3 days of selection after 4F infection, the RNA was sequenced. We used k-means clustering to divide genes that change upon 4F expression, and then we further subdivided each cluster for changes by the further loss of *Rb* (Figure 3A, Figures S3C and S3D, Table S1 available online). In all these clusters, loss of *Rb* led to changes in the expression of cell cycle genes. However, both positive (e.g., *Mcm3*, *Pola1*, and *Cdk1*) and negative (e.g., *p107*, *Cdkn2c*, and *Brca1*) cell cycle regulators were upregulated, which may explain why loss of Rb function does not promote cell division under these conditions (Figures 3A, Figure S3C and S3D). We used gene set enrichment analysis (GSEA) to determine the consequences of *Rb* deletion on MEF or iPSC gene sets. We found a significant enrichment for the iPSC-specific gene signature in cells without *Rb* compared to *Rb* wild-type cells upon 4F expression (Figure 3B and Table S1). Interestingly, using RT-qPCR, we observed a small but significant increase in *Sox2* and *Oct4* expression in *Rb*-deficient MEFs even without 4F infection (Figure 3C). As expected, the absolute expression of pluripotency genes was still much lower (<0.5%) than in ESCs (Figure 3D). Loss of the entire Rb family did not further increase the expression of these pluripotency genes, in contrast to cell cycle genes (Figures 1D and 3C). Slight *OCT4* and *SOX2* induction was also observed in human cells in response to *RB* knockdown (Figure 3E). Flow cytometry of *Sox2-GFP* MEFs after acute knockdown of *Rb* showed that the *Sox2* induction observed in bulk analysis is caused by slight induction in many cells and not strong induction in a few cells (Figure 3F). Thus, loss of *Rb* leads to a global derepression of components of the pluripotency transcriptional program, leading to only a subtle gene induction in the majority of cells.

To determine if the repressive action of Rb on pluripotency genes might be direct, we performed Rb chromatin immunoprecipitation (ChIP) assays under the same conditions as the RNA sequencing profiling. Interrogating a few selected genomic regions by ChIP-qPCR, we observed that Rb binds to the promoter regions of *Sox2* and *Oct4* as well as classical cell cycle genes (Figure 4A). Global analysis of Rb ChIP sequencing data showed that the

majority of the genes identified as being bound by Rb are associated with the cell cycle and most are upregulated upon loss of *Rb*, consistent with its established role as a transcriptional repressor (Figure S4A and S4B). Genome-wide data also confirmed robust Rb binding at the *Sox2* and *Oct4* loci (Figure 4B, Table S2). Moreover, we found Rb binding to the regulatory regions of a number of genes involved in reprogramming and pluripotency, an observation supported by the analysis of human Rb ChIP sequencing data sets (Chicas et al., 2010) (Figure S4C). Remarkably, at the *Sox2* locus, Rb was primarily bound to the downstream enhancer (SRR2; Figure 4B and Figure S4D), the active enhancer in pluripotent lineages (Tomioka et al., 2002).

We next sought to determine if binding of Rb to pluripotency genes might play a role in a developmental context. When we examined expression data of both wild-type and *Rb* family mutant mouse ESCs before and after differentiation into embryoid bodies (EBs), we found a significant defect in the silencing of pluripotency genes (listed in Figure S4C) upon differentiation (Figures 4C and 4D). Additionally, Rb progressively binds to both *Oct4* and *Sox2* during EB differentiation, correlating with their silencing (Figure 4E). Together, these experiments indicate that the binding of Rb to pluripotency factors, including *Sox2* and *Oct4*, may both contribute to their silencing in differentiated cells and restrict their re-expression during the reprogramming process.

Because Rb typically requires a binding partner to be recruited to DNA, we sought to investigate how Rb is localized to pluripotency genes. Previous studies have suggested that E2F proteins bind to *Sox2* and *Oct4* (Julian et al., 2013; Xu et al., 2007). To explore if direct interactions between Rb and E2Fs at these loci were involved in gene repression, we used MEFs in which mutations at either the E2F-binding pocket (ΔG allele) or the LxCxE-binding cleft (ΔL allele) were knocked in to the endogenous *Rb* locus (Figure 4F) (Isaac et al., 2006; Talluri et al., 2010). We found a specific increase in the reprogramming efficiency of DG mutants (Figure 4G), correlating with increased levels of *Oct4* and *Sox2* (Figure 4H), similar to *Rb* deletion (Figure 3C). Thus, interactions through the E2F-binding pocket are required for the silencing of pluripotency genes by Rb.

Rb Contributes to the Maintenance of the Chromatin State at Pluripotency Genes in Fibroblasts

Based on these observations and the known interactions between Rb and regulators of chromatin structure (Longworth and Dyson, 2010), we determined whether loss of Rb function affects the chromatin at pluripotency genes. At both *Oct4* and *Sox2*, we observed a significant increase in the acetylation of histone H3 (H3Ac) in the proximal promoter regions upon loss of Rb (Figure S5A). The extent of this increase was similar to what we observed for Rb canonical targets such as *Ccna2* (Figure S5A). However, H3K4me3 was not increased at the *Oct4* or *Sox2* promoter, unlike at *Ccna2*, which may reflect the difference between enhanced gene activation of an already expressed E2F target upon *Rb* loss and the slight increase of basal transcription that we observed for *Oct4* and *Sox2* (Figures 3C and 3D). Additionally, we found a significant loss of H3K27me3 at *Oct4* (Figure S5A).

Using ChIP sequencing to gain a genome-wide perspective on histone changes upon *Rb* loss, we detected significantly increased levels of both H3Ac and H4K4me3 and a decrease of

H3K27me3 at multiple pluripotency genes, including *Oct4*, *Nanog*, and *Sox2* (Figure 5A, Figure S5B). Increased activating marks including H3Ac and H3K4me3 were highly correlated (Figure S5C) and found predominantly at cell cycle genes and known Rb targets such as *p107* (Figure 5A, Table S3); however, increased activating marks were also observed at both *Sox2* and *Nanog* (Figure 5A). Notably, the region with increased H3Ac and H3K4me3 downstream of *Sox2* is not the SRR2 enhancer, but rather a region that is bound by both p300 and CTCF and can interact with the SRR2 enhancer (Dixon et al., 2012). GSEA indicated that an iPSC-specific gene set is significantly enriched among the genes that gain H3Ac and H3K4me3 to a similar degree as a gene set specific for Rb loss (Figure 5B).

A recent study described the existence of broad H3K4me3 domains that mark genes essential for cell identity and function (Benayoun et al., 2014). We observed a change in broad domain organization upon loss of *Rb* (Figure 5C, Figures S5D and S5E). Strikingly, an unbiased analysis of genes that showed increased H3K4me3 domain breadth showed that these genes were enriched to be direct transcriptional targets of the core pluripotency network (e.g., OCT4 and NANOG; Table S3). The same enrichment for transcriptional targets of OCT4, SOX2, KLF4, NANOG, and TCF3 was observed in Rb-deficient cells when we analyzed increases in H3K4me3 breadth specifically in the set of H3K4me3-marked genes (Figure 5D). Peaks broadened by loss of *Rb* were domains more likely to be in the top 5% broadest domains in mouse ESCs (Figures 5E and 5F). Thus, the absence of Rb in MEFs generates a chromatin landscape that more closely resembles that of an ESC. Thus, Rb loss not only leads to derepression of some core pluripotency genes, but also specifically alters the chromatin of downstream targets for these pluripotency factors, possibly facilitating the transcription of a global pluripotency program and its implementation.

The silencing of chromatin at key pluripotency genes by Rb is consistent with the known interactions of Rb with key repressors (Longworth and Dyson, 2010). To interrogate the recruitment of such factors to *Oct4* and *Sox2*, we performed ChIP experiments in *Rb* wild-type and mutant MEFs. These experiments showed a strong correlation between cofactor recruitment and the histone mark changes observed. As mentioned above, *Rb* loss decreased H3K27me3 at a region spanning the distal enhancers to the promoter of *Oct4* (Figure 5A), which correlated with a decrease of EZH2 recruitment to this region (Figure 5G). The increased H3Ac at the proximal promoters of *Oct4* and *Sox2* observed in *Rb* mutant cells by ChIP-qPCR (Figure S5A) corresponded to a significant decrease of HDAC recruitment to these loci (Figures 5G and 5H). It should be noted, however, that the change in H3Ac at the proximal promoters of *Oct4* and *Sox2* was not identified by ChIP-eq, presumably due to the low levels of this mark escaping detection when analyzed on a genomic scale. Finally, because p27 was reported to repress *Sox2* (Li et al., 2012), we determined p27 localization at the DNA in wild-type, $p130^{-/-}$; $p107^{-/-}$, and *Rb* family TKO MEFs. We found p27 binding to the downstream enhancer of *Sox2* even in the absence of *p130* and *p107*, but not in the TKO MEFs, indicating that the recruitment of p27 at the *Sox2* locus can also be mediated by Rb (Figure S5F).

Rb Functionally Regulates *Oct4* and *Nanog*, and Its Loss Can Functionally Replace *Sox2* in Reprogramming

While the levels of derepression of pluripotency genes observed in Rb-deficient fibroblasts are small, we wondered if they may be sufficient to bypass the need for exogenous reprogramming factors. We infected *Oct4-Neo*^{R} MEFs with three-factor combinations of the reprogramming factors and a hairpin against *Rb*. With just *Oct4, Klf4*, and *c-Myc*, several neomycin-resistant clones were readily obtained in *Rb* knockdown cells, but not in control cells. Fewer clones were observed with *Oct4* and *Klf4* alone in the *Rb* knockdown than with *c-Myc* or all four factors (Figure S6A and S6B). No iPSC colonies were observed when either *Klf4* or *Oct4* were omitted. These Rb^{KD} OKM clones, in which the absence of *Sox2* transgene was verified (Figure S6C and S6D), had a similar morphology to that of iPSCs reprogrammed with the four factors and expressed endogenous *Oct4, Sox2, Nanog*, and AP activity (Figure 6A). Additionally the *Rb*-deficient iPSCs reprogrammed without *Sox2* formed teratomas with all three germ layers (Figure S6E) and contributed to a host embryo forming chimeric mice (Figure S6F). Thus, acute loss of *Rb* can functionally replace *Sox2* during iPSC reprogramming.

To determine whether Rb could control the expression of pluripotency factors beyond *Sox2*, using another system, we tested if *Rb* loss might prime *Oct4* and *Nanog* for activation. We employed the CRISPR-on approach (Cheng et al., 2013) to directly target the transcriptional activator VP64 to the *Oct4* and *Nanog* promoters and observed a significantly enhanced expression from these genes when *Rb* was absent (Figure 6B). Therefore, while *Rb* loss did not compensate for exogenous *Oct4* to generate fully reprogrammed iPSCs, Rb regulates the *Oct4* locus physiologically.

Sox2 Is Required for the Development of Tumors Initiated by Loss of *Rb*

Based on emerging evidence that *Sox2* plays oncogenic roles (Lu et al., 2010; Rudin et al., 2012), we determined if the derepression of *Sox2* observed in *Rb*-deficient cells might be relevant to cancer initiation. To test this idea, we crossed *Rosa26*^{CreER} *Rb*$^{lox/lox}$ mice to *Sox2*$^{lox/lox}$ mice. As expected (Jacks et al., 1992), we observed a significantly enlarged pituitary at 9 weeks after tamoxifen injection in *Rosa26*^{CreER} *Rb*$^{lox/lox}$ mice. Strikingly, concomitant loss of *Sox2* completely blocked this cancer phenotype (Figures 6C and 6D), independent of gender (Figure S6G and S6H). Accordingly, loss of *Sox2* completely inhibited cell proliferation in the pituitary of *Rb*-mutant mice (Figures 6E and 6F, Figure S6I). These experiments indicate that *Sox2* is critical for cancer initiation upon loss of *Rb* in the mouse pituitary gland.

DISCUSSION

The retinoblastoma tumor suppressor Rb is commonly inactivated in human cancer. While Rb has been extensively studied, its mechanisms of action remain incompletely understood. Here, using iPSC reprogramming as a cellular system, we identified a new facet of Rb tumor suppressor function in which Rb restricts the expression of pluripotency genes and their downstream targets, thereby preventing cellular dedifferentiation and transformation.

The degree of Rb involvement in direct regulation of pluripotency genes and downstream targets is particularly noteworthy. Although on the individual gene level, the transcriptional changes in pluripotency networks observed after Rb inactivation are subtle, a sizeable number of genes are affected. The genome-wide summation of these individually small effects results in a global transcriptionally permissive state and could explain the increased cell pliability of *Rb*-deficient cells that was observed before (Calo et al., 2010; McEvoy et al., 2011). In fact, that low levels of pluripotency genes, particularly *Sox2*, may have strong phenotypic effects is not surprising because iPSCs often have few genomic integrations of *Sox2* proviruses (Meissner et al., 2007; Wernig et al., 2007), and low *Sox2* is in fact favorable for high-quality iPSCs (Carey et al., 2011). Our findings also provide a molecular basis for related cellular phenotypes directly or indirectly involving Rb and previously assumed to be caused by changes in the cell cycle (Banito et al., 2009; Li et al., 2010; Liu et al., 2009). Notably, the effect on reprogramming was specific for Rb and was not observed for the closely related genes *p107* and *p130*. Much like Rb, both of these factors restrict cell cycle progression (Dannenberg et al., 2000; Sage et al., 2000), yet are rarely mutated in cancer. Therefore, the unique ability of Rb among its family members to suppress dedifferentiation may provide an explanation for its crucial role in suppressing cancer formation while its cell cycle checkpoint role is compensated more potently by the usually intact p107 and p130 proteins.

We found that the regulation of target genes by Rb correlates with the recruitment of histone modifying complexes and the subsequent regulation of histone marks. While loss of *Rb* resulted in increases of H3Ac and H3K4me3 at cell cycle genes, pluripotency genes, including *Oct4*, *Sox2*, and *Nanog*, mostly gained H3Ac and lost H3K27me3. This effect of *Rb* loss on pluripotency genes therefore more likely represents a derepression resulting in increased basal transcription rather than full activation, which is associated with robust promoter H3K4me3. While this derepression is general to pluripotency genes, we know that not all genes respond to the same degree because the increase of total expression of *Sox2* is markedly higher than that of *Oct4*, and Rb loss could only replace *Sox2* and not *Oct4* to derive iPSCs. This may be explained by additional regulatory mechanisms restricting *Oct4* expression, including high levels of DNA methylation at the *Oct4* locus (Mikkelsen et al., 2008), or a lack of $LIN28^{+}$ regulation of *Oct4* mRNA in MEFs (Qiu et al., 2010). Nevertheless, loss of *Rb* enhances the expression of both *Oct4* and *Nanog* when forced by a strong transcriptional activator, supporting a direct role for *Rb* in the regulation of these genes. Additional evidence linking cell cycle regulators to pluripotency genes is starting to emerge. For instance, the Cdk2 inhibitor p27 also controls the pluripotency of ESCs by direct inhibition of *Sox2* (Li et al., 2012) (see also below). This regulation is mediated by the same enhancer that we found to be bound and regulated by Rb, suggesting possible interactions between p27 and Rb on the chromatin. Future studies may elucidate whether such interactions exist genome-wide or are specific for this enhancer.

While we observed changes in the chromatin landscape of MEFs after *Rb* loss, we expected that perturbation of the LxCxE binding cleft would have a reprogramming phenotype similar to loss of *Rb*. Mice harboring these knockin mutations have shown defects in chromatin modifications in other settings (Bourgo et al., 2011; Talluri et al., 2010). However, our data

show that interactions through this surface are not required for the silencing of *Sox2* and *Oct4*. This is consistent with reports that in differentiated tissues, *Rb*-dependent silencing is normal in LxCxE mutant mice (Andrusiak et al., 2013; Talluri et al., 2010). Furthermore, a dominant-negative DP1 (which blocks E2F transactivation) can rescue increased acetylation observed upon *Rb* loss (Andrusiak et al., 2013). This presents two models whereby *Rb* might regulate heterochromatin. First, HDACs interact with Rb in LxCxE-in-dependent ways, so the longstanding model of direct HDAC recruitment is correct but at least partly LxCxE independent. Alternatively, Rb repression of E2Fs allows HDAC recruitment through other neighboring contacts. In this way, the effects on chromatin are genetically Rb dependent but the biochemical mechanism is distinct from simply being recruited by Rb. Regardless of which paradigm explains our data, E2F appears to be central to the mechanism of Rb regulation of *Sox2* and *Oct4*.

Regulation of *Sox2* at its upstream enhancer by the Rb family/ E2F and at its downstream enhancer by p21 has already been shown to direct the fate choices of neural stem cells (Julian et al., 2013; Marqués-Torrejón et al., 2013). We observe that Rb represses *Sox2* at its downstream, pluripotency-specific enhancer as cells differentiate. Moreover, the loss of this repression in the pituitary induces hyperplasia in a *Sox2*-dependent manner. It is noteworthy that *Sox2* is expressed in the retina (Li et al., 2012), in which loss of Rb is tumor initiating. Amplification of *Sox2* has also been shown to be a driver mutation in human small cell lung cancer, a cancer initiated by loss of *RB* and *p53* (Rudin et al., 2012). Although inactivation of Rb, by either mutation or repression, is common to nearly all cancers, it is only initiating in a few cell types. This difference may rely in part on the initiating cell's ability to reactivate *Sox2* transcriptional networks. The extent by which *Rb* regulation of *Sox2* limits tumors in humans is still unknown, but our observations support the idea that cellular reprogramming assays can be used as a cellular system to probe the molecular mechanisms of cancer initiation.

EXPERIMENTAL PROCEDURES

Cell Lines

The cell lines used were as follows: $Rb^{lox/lox}$ (cKO), $Oct4\text{-}GFP^{+/-}$, $Oct4\text{-}Neo^{+/-}$, B6;129S-$Sox2^{tm2Hoch}$/J (*Sox2-GFP*) and $M2rtTA^{+/-}$;$Oct4\text{-}GFP^{+/-}$ (Brambrink et al., 2008; Burkhart et al., 2010a; Meissner et al., 2007; Wernig et al., 2007). $Rb1^{\Delta L/\Delta L}$ MEFs have been reported previously (Isaac et al., 2006). $Rb1^{\Delta G/\Delta G}$ MEFs express an R461E, K542E mutant and its properties have previously been reported (Cecchini and Dick, 2011; Cecchini et al., 2014).

Reprogramming and Differentiation Assays

For the 96-well efficiency assays, shRNA-infected cells were selected by 3 days of growth in puromycin, infected with the 4F, and plated at a density of 100 cells per well into 96-well plates containing 1,000 g-irradiated feeder cells per well. Wells with AP^+ cells and proper morphology (after 15 days) were reported to remove potential contribution of the seeding of daughter colonies. EBs were formed when we plated trypsinized ESCs in nonadherent plates at a density of 5.5×10^5 cells/ml in DMEM with 10% serum. After 3 days they were plated

onto gelatin-coated tissue culture plates. After 5 days they were maintained in serum free conditions.

CFSE Analysis

CFSE staining was performed using the CellTrace™ Violet Cell Proliferation Kit (Invitrogen #C34557). Cells were trypsinized and washed with PBS, and then CFSE was added to 5 μM. They were incubated in the dark at 37°C for 20 min and then the reaction was quenched with media for 5 min. The cells were then washed, cultured, and later analyzed by FACS.

RNA and ChIP Sequencing

ChIP was performed as previously described (Burkhart et al., 2010b). Antibodies are listed in Table S5. Sequencing libraries were generated using the NEBNext DNA Sample Prep Master Mix Set (New England Biolabs) and purified using Agencourt Ampure XP beads (Beckman Coulter). Library quality was assessed on an Agilent 2100 Bioanalyzer and sequenced to generate single-end 50 bp reads using the Illumina HiSeq platform. We analyzed ChIP data by mapping the reads using Bowtie2 and identified peaks using MACS2 for the histone ChIP sequencing and CisGenome for the Rb ChIP. For expressional profiling, purified RNA was processed into cDNA with the Ovation RNA-Seq System V2 (NuGEN) and sonicated using a Covaris S2 Sonicator. RNA sequencing data were analyzed with the Tuxedo suite. H3K4me3 breadth remodeling was performed as previously described (Benayoun et al., 2014). See Supplemental Experimental Procedures for additional information.

Pituitary Sectioning and Staining

To isolate the pituitary, we fixed the whole head overnight in Bouin's Fixative, removed it, fixed it overnight in 4% paraformaldehyde, and then dehydrated it in 70% ethanol. Antigen retrieval on the sections was performed using the Trilogy solution (Cell Marque) for 15 min in a pressure cooker. The sections were then washed in PBS + Tween20 (PBST) and fixed for 1 hr in PBST with 10% normal horse serum (NHS). They were incubated with Ki67 antibody (Table S5) overnight at 4°C in PBST with 5% NHS. After being washed in PBS, they were incubated with the secondary antibody in PBS with 5% NHS. Sections were then washed with PBS, stained with DAPI, and mounted. We identified cells by using CellProfiler (http://www.cellprofiler.org) to count nuclei on the DAPI channel, while Ki67 was scored manually in a blinded manner.

Supplementary Material

Refer to Web version on PubMed Central for supplementary material.

ACKNOWLEDGMENTS

We would like to thank Gary Mantalas, Ben Passarelli, and Steven Quake for sequencing; Helen Blau for critical reading of the manuscript; Moritz Mall for the CRISPR vectors; and Jamie Imam for assistance with teratoma assays. This work was supported by PHS Grant #T32 CA09151, awarded by the NCI; DHHS (M.S.K.); the Spectrum Child Health Child Health Research Institute (M.S.K.); CIHR MD/PhD (M.J.C.); the Lucile Packard Foundation for Children's Health (J.S.); and the CIRM (CIRM RB1-01385 -J.S.). F.A.D. is the Wolfe Senior

Fellow in Tumor Suppressor Genes at Western University, M.W. is a New York Stem Cell Foundation-Robertson Investigator and a Tashia and John Morgridge Faculty Scholar, and J.S. is the Harriet and Mary Zelencik Scientist in Children's Cancer and Blood Diseases.

REFERENCES

Andrusiak MG, Vandenbosch R, Dick FA, Park DS, Slack RS. LXCXE-independent chromatin remodeling by Rb/E2f mediates neuronal quiescence. Cell Cycle. 2013; 12:1416–1423. [PubMed: 23574720]

Banito A, Rashid ST, Acosta JC, Li S, Pereira CF, Geti I, Pinho S, Silva JC, Azuara V, Walsh M, et al. Senescence impairs successful reprogramming to pluripotent stem cells. Genes Dev. 2009; 23:2134–2139. [PubMed: 19696146]

Batista LF, Pech MF, Zhong FL, Nguyen HN, Xie KT, Zaug AJ, Crary SM, Choi J, Sebastiano V, Cherry A, et al. Telomere shortening and loss of self-renewal in dyskeratosis congenita induced pluripotent stem cells. Nature. 2011; 474:399–402. [PubMed: 21602826]

Benayoun BA, Pollina EA, Ucar D, Mahmoudi S, Karra K, Wong ED, Devarajan K, Daugherty AC, Kundaje AB, Mancini E, et al. H3K4me3 breadth is linked to cell identity and transcriptional consistency. Cell. 2014; 158:673–688. [PubMed: 25083876]

Bourgo RJ, Thangavel C, Ertel A, Bergseid J, McClendon AK, Wilkens L, Witkiewicz AK, Wang JY, Knudsen ES. RB restricts DNA damage-initiated tumorigenesis through an LXCXE-dependent mechanism of transcriptional control. Mol. Cell. 2011; 43:663–672. [PubMed: 21855804]

Brambrink T, Foreman R, Welstead GG, Lengner CJ, Wernig M, Suh H, Jaenisch R. Sequential expression of pluripotency markers during direct reprogramming of mouse somatic cells. Cell Stem Cell. 2008; 2:151–159. [PubMed: 18371436]

Burkhart DL, Sage J. Cellular mechanisms of tumour suppression by the retinoblastoma gene. Nat. Rev. Cancer. 2008; 8:671–682. [PubMed: 18650841]

Burkhart DL, Ngai LK, Roake CM, Viatour P, Thangavel C, Ho VM, Knudsen ES, Sage J. Regulation of RB transcription in vivo by RB family members. Mol. Cell. Biol. 2010a; 30:1729–1745. [PubMed: 20100864]

Burkhart DL, Wirt SE, Zmoos AF, Kareta MS, Sage J. Tandem E2F binding sites in the promoter of the p107 cell cycle regulator control p107 expression and its cellular functions. PLoS Genet. 2010b; 6:e1001003. [PubMed: 20585628]

Calo E, Quintero-Estades JA, Danielian PS, Nedelcu S, Berman SD, Lees JA. Rb regulates fate choice and lineage commitment in vivo. Nature. 2010; 466:1110–1114. [PubMed: 20686481]

Carey BW, Markoulaki S, Hanna JH, Faddah DA, Buganim Y, Kim J, Ganz K, Steine EJ, Cassady JP, Creyghton MP, et al. Reprogramming factor stoichiometry influences the epigenetic state and biological properties of induced pluripotent stem cells. Cell Stem Cell. 2011; 9:588–598. [PubMed: 22136932]

Cecchini MJ, Dick FA. The biochemical basis of CDK phosphorylation-independent regulation of E2F1 by the retinoblastoma protein. Biochem. J. 2011; 434:297–308. [PubMed: 21143199]

Cecchini MJ, Thwaites MJ, Talluri S, MacDonald JI, Passos DT, Chong JL, Cantalupo P, Stafford PM, Saenz-Robles MT, Francis SM, et al. A retinoblastoma allele that is mutated at its common E2F interaction site inhibits cell proliferation in gene-targeted mice. Mol. Cell Biol. 2014; 34:2029–2045. [PubMed: 24662053]

Cheng AW, Wang H, Yang H, Shi L, Katz Y, Theunissen TW, Rangarajan S, Shivalila CS, Dadon DB, Jaenisch R. Multiplexed activation of endogenous genes by CRISPR-on, an RNA-guided transcriptional activator system. Cell Res. 2013; 23:1163–1171. [PubMed: 23979020]

Chicas A, Wang X, Zhang C, McCurrach M, Zhao Z, Mert O, Dickins RA, Narita M, Zhang M, Lowe SW. Dissecting the unique role of the retinoblastoma tumor suppressor during cellular senescence. Cancer Cell. 2010; 17:376–387. [PubMed: 20385362]

Chinnam M, Goodrich DW. RB1, development, and cancer. Curr. Top. Dev. Biol. 2011; 94:129–169. [PubMed: 21295686]

Conklin JF, Sage J. Keeping an eye on retinoblastoma control of human embryonic stem cells. J. Cell. Biochem. 2009; 108:1023–1030. [PubMed: 19760644]

Dannenberg JH, van Rossum A, Schuijff L, te Riele H. Ablation of the retinoblastoma gene family deregulates G(1) control causing immortalization and increased cell turnover under growth-restricting conditions. Genes Dev. 2000; 14:3051–3064. [PubMed: 11114893]

Dixon JR, Selvaraj S, Yue F, Kim A, Li Y, Shen Y, Hu M, Liu JS, Ren B. Topological domains in mammalian genomes identified by analysis of chromatin interactions. Nature. 2012; 485:376–380. [PubMed: 22495300]

Goding CR, Pei D, Lu X. Cancer: pathological nuclear reprogramming? Nat. Rev. Cancer. 2014; 14:568–573. [PubMed: 25030952]

Hanna J, Saha K, Pando B, van Zon J, Lengner CJ, Creyghton MP, van Oudenaarden A, Jaenisch R. Direct cell reprogramming is a stochastic process amenable to acceleration. Nature. 2009; 462:595–601. [PubMed: 19898493]

Hochedlinger K, Yamada Y, Beard C, Jaenisch R. Ectopic expression of Oct-4 blocks progenitor-cell differentiation and causes dysplasia in epithelial tissues. Cell. 2005; 121:465–477. [PubMed: 15882627]

Isaac CE, Francis SM, Martens AL, Julian LM, Seifried LA, Erdmann N, Binné UK, Harrington L, Sicinski P, Bérubé NG, et al. The retinoblastoma protein regulates pericentric heterochromatin. Mol. Cell. Biol. 2006; 26:3659–3671. [PubMed: 16612004]

Jacks T, Fazeli A, Schmitt EM, Bronson RT, Goodell MA, Weinberg RA. Effects of an Rb mutation in the mouse. Nature. 1992; 359:295–300. [PubMed: 1406933]

Julian LM, Vandenbosch R, Pakenham CA, Andrusiak MG, Nguyen AP, McClellan KA, Svoboda DS, Lagace DC, Park DS, Leone G, et al. Opposing regulation of Sox2 by cell-cycle effectors E2f3a and E2f3b in neural stem cells. Cell Stem Cell. 2013; 12:440–452. [PubMed: 23499385]

Koche RP, Smith ZD, Adli M, Gu H, Ku M, Gnirke A, Bernstein BE, Meissner A. Reprogramming factor expression initiates widespread targeted chromatin remodeling. Cell Stem Cell. 2011; 8:96–105. [PubMed: 21211784]

Krizhanovsky V, Lowe SW. Stem cells: The promises and perils of p53. Nature. 2009; 460:1085–1086. [PubMed: 19713919]

Li F, He Z, Shen J, Huang Q, Li W, Liu X, He Y, Wolf F, Li CY. Apoptotic caspases regulate induction of iPSCs from human fibroblasts. Cell Stem Cell. 2010; 7:508–520. [PubMed: 20887956]

Li H, Collado M, Villasante A, Matheu A, Lynch CJ, Cañamero M, Rizzoti K, Carneiro C, Martínez G, Vidal A, et al. p27(Kip1) directly represses Sox2 during embryonic stem cell differentiation. Cell Stem Cell. 2012; 11:845–852. [PubMed: 23217425]

Liu Y, Clem B, Zuba-Surma EK, El-Naggar S, Telang S, Jenson AB, Wang Y, Shao H, Ratajczak MZ, Chesney J, Dean DC. Mouse fibroblasts lacking RB1 function form spheres and undergo reprogramming to a cancer stem cell phenotype. Cell Stem Cell. 2009; 4:336–347. [PubMed: 19341623]

Longworth MS, Dyson NJ. pRb, a local chromatin organizer with global possibilities. Chromosoma. 2010; 119:1–11. [PubMed: 19714354]

Lu Y, Futtner C, Rock JR, Xu X, Whitworth W, Hogan BL, Onaitis MW. Evidence that SOX2 overexpression is oncogenic in the lung. PLoS ONE. 2010; 5:e11022. [PubMed: 20548776]

Manning AL, Dyson NJ. RB: mitotic implications of a tumour suppressor. Nat. Rev. Cancer. 2012; 12:220–226. [PubMed: 22318235]

Marqués-Torrejón MA, Porlan E, Banito A, Gómez-Ibarlucea E, Lopez-Contreras AJ, Ferná ndez-Capetillo O, Vidal A, Gil J, Torres J, Fariñas I. Cyclin-dependent kinase inhibitor p21 controls adult neural stem cell expansion by regulating Sox2 gene expression. Cell Stem Cell. 2013; 12:88–100. [PubMed: 23260487]

McEvoy J, Flores-Otero J, Zhang J, Nemeth K, Brennan R, Bradley C, Krafcik F, Rodriguez-Galindo C, Wilson M, Xiong S, et al. Coexpression of normally incompatible developmental pathways in retinoblastoma genesis. Cancer Cell. 2011; 20:260–275. [PubMed: 21840489]

Meissner A, Wernig M, Jaenisch R. Direct reprogramming of genetically unmodified fibroblasts into pluripotent stem cells. Nat. Biotechnol. 2007; 25:1177–1181. [PubMed: 17724450]

Mikkelsen TS, Hanna J, Zhang X, Ku M, Wernig M, Schorderet P, Bernstein BE, Jaenisch R, Lander ES, Meissner A. Dissecting direct reprogramming through integrative genomic analysis. Nature. 2008; 454:49–55. [PubMed: 18509334]

Nakagawa M, Koyanagi M, Tanabe K, Takahashi K, Ichisaka T, Aoi T, Okita K, Mochiduki Y, Takizawa N, Yamanaka S. Generation of induced pluripotent stem cells without Myc from mouse and human fibroblasts. Nat. Biotechnol. 2008; 26:101–106. [PubMed: 18059259]

Nicolay BN, Dyson NJ. The multiple connections between pRB and cell metabolism. Curr. Opin. Cell Biol. 2013; 25:735–740. [PubMed: 23916769]

Park IH, Zhao R, West JA, Yabuuchi A, Huo H, Ince TA, Lerou PH, Lensch MW, Daley GQ. Reprogramming of human somatic cells to pluripotency with defined factors. Nature. 2008; 451:141–146. [PubMed: 18157115]

Qiu C, Ma Y, Wang J, Peng S, Huang Y. Lin28-mediated post-transcriptional regulation of Oct4 expression in human embryonic stem cells. Nucleic Acids Res. 2010; 38:1240–1248. [PubMed: 19966271]

Rudin CM, Durinck S, Stawiski EW, Poirier JT, Modrusan Z, Shames DS, Bergbower EA, Guan Y, Shin J, Guillory J, et al. Comprehensive genomic analysis identifies SOX2 as a frequently amplified gene in small-cell lung cancer. Nat. Genet. 2012; 44:1111–1116. [PubMed: 22941189]

Sage J, Mulligan GJ, Attardi LD, Miller A, Chen S, Williams B, Theodorou E, Jacks T. Targeted disruption of the three Rb-related genes leads to loss of G(1) control and immortalization. Genes Dev. 2000; 14:3037–3050. [PubMed: 11114892]

Sarkar A, Hochedlinger K. The sox family of transcription factors: versatile regulators of stem and progenitor cell fate. Cell Stem Cell. 2013; 12:15–30. [PubMed: 23290134]

Talluri S, Isaac CE, Ahmad M, Henley SA, Francis SM, Martens AL, Bremner R, Dick FA. A G1 checkpoint mediated by the retinoblastoma protein that is dispensable in terminal differentiation but essential for senescence. Mol. Cell. Biol. 2010; 30:948–960. [PubMed: 20008551]

Tomioka M, Nishimoto M, Miyagi S, Katayanagi T, Fukui N, Niwa H, Muramatsu M, Okuda A. Identification of Sox-2 regulatory region which is under the control of Oct-3/4-Sox-2 complex. Nucleic Acids Res. 2002; 30:3202–3213. [PubMed: 12136102]

Viatour P, Sage J. Newly identified aspects oftumor suppression by RB. Dis. Model. Mech. 2011; 4:581–585. [PubMed: 21878458]

Wernig M, Meissner A, Foreman R, Brambrink T, Ku M, Hochedlinger K, Bernstein BE, Jaenisch R. In vitro reprogramming of fibroblasts into a pluripotent ES-cell-like state. Nature. 2007; 448:318–324. [PubMed: 17554336]

Wernig M, Meissner A, Cassady JP, Jaenisch R. c-Myc is dispensable for direct reprogramming of mouse fibroblasts. Cell Stem Cell. 2008; 2:10–12. [PubMed: 18371415]

Xu X, Bieda M, Jin VX, Rabinovich A, Oberley MJ, Green R, Farnham PJ. A comprehensive ChIP-chip analysis of E2F1, E2F4, and E2F6 in normal and tumor cells reveals interchangeable roles of E2F family members. Genome Res. 2007; 17:1550–1561. [PubMed: 17908821]

Highlights

- The Rb tumor suppressor inhibits reprogramming of fibroblasts to iPSCs
- The effect of Rb on reprogramming is independent of cell-cycle regulation
- Rb promotes assembly of repressive chromatin at pluripotency network genes
- Deletion of *Sox2* prevents cancer initiation upon loss of Rb in mice

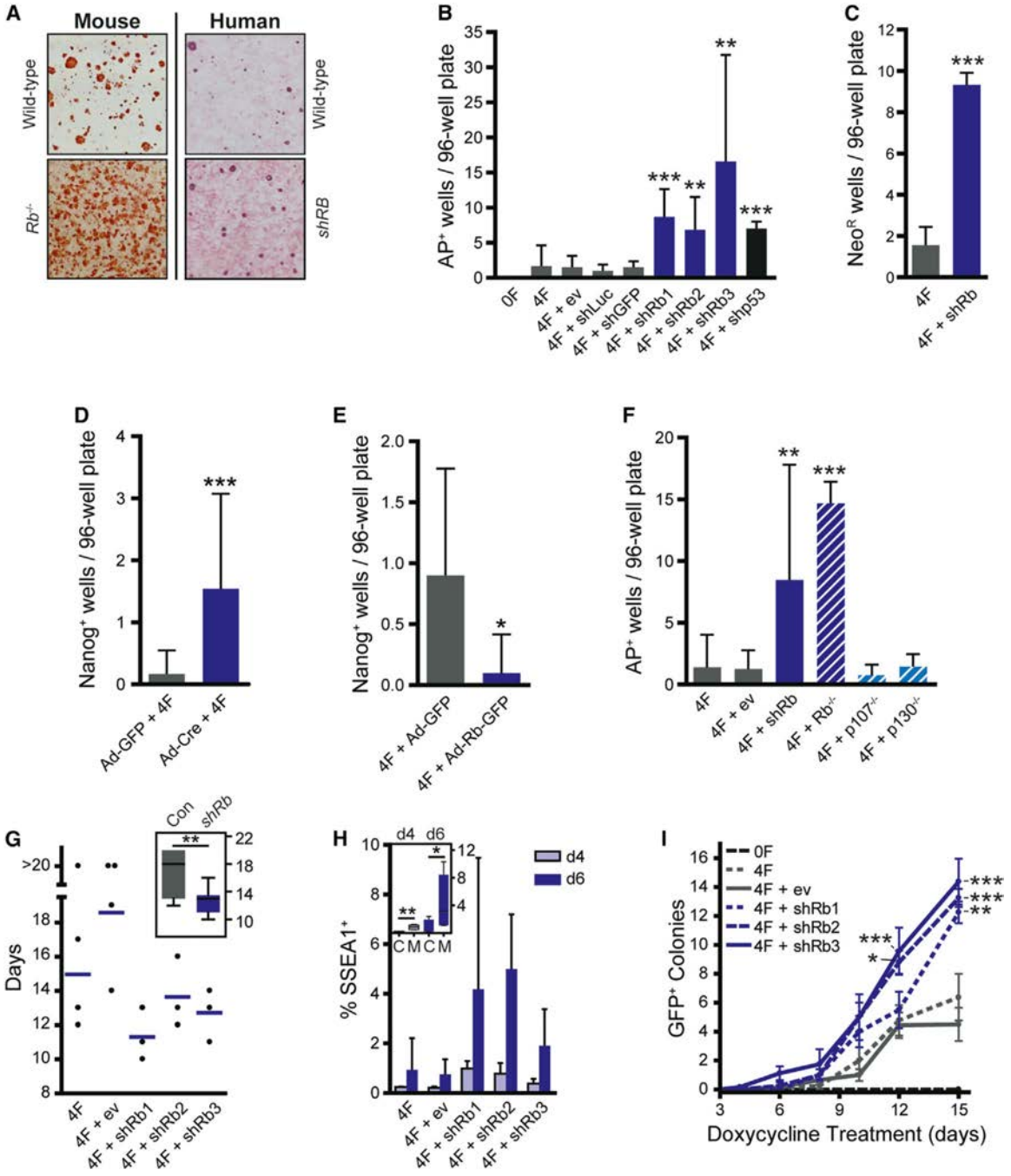

Figure 1. Rb Loss Removes a Block to the Cellular Reprogramming of iPSCs

(A) Reprogramming of early-passage mouse and human fibroblasts. Rb was depleted by either a germline mutation (mouse)or shRNA knockdown (human). Cells were infected with 4F and stained for AP activity after 14 or 30 days in culture, respectively. Representative images are shown.

(B) Wells with AP^+ cells and proper morphology from *Oct4-GFP* MEFs with lentiviral constructs expressing hairpins to *Rb*, *p53*, *GFP*, *Luciferase*, or an empty vector (ev),

subjected to the 4F (see Experimental Procedures). Significance was assessed by a t test to the 4F-infected sample ($n \geq 3$).

(C) Efficiency of iPSC formation was tested using *Oct4-Neo*^{R} MEFs followed by treatment with G418 on day 15 and AP staining after 5 days of selection. Significance was assessed by a t test to the 4F sample.

(D) Efficiency of iPSC formation was tested using cKO MEFs stained for AP activity and *Nanog* expression to identify iPSC colonies. Significance was assessed by a t test ($n = 3$).

(E) Efficiency of iPSC formation was tested with *Rb* overexpression by infection with Ad-Rb-GFP or Ad-GFP. Significance was assessed by a t test ($n = 2$).

(F) Efficiency was tested for *Rb* knockdown MEFs and knockout MEFs for each of the pocket proteins. Significance was assessed by a t test to the 4F sample ($n \geq 3$).

(G) Kinetics of reprogramming was determined by infecting shRb-infected *Oct4-GFP* MEFs with 4F. Plates were scored by the earliest GFP$^+$ colony appearance up to day 20. Significance was assessed by a t test comparing the controls against the three shRb hairpins ($n \geq 3$).

(H) Analysis of early reprogramming events by SSEA1 expression in shRb (M) or control (C) infected MEFs 4 and 6 days after 4F ($n = 3$).

(I) Dox-dependence assay where shRb-infected *Oct4-GFP* MEFs were infected with 4F on day 0 and treated with Dox on day 1. The cells were switched to Dox-free media at regular intervals and GFP$^+$ colonies were screened on day 15 ($n \geq 3$).

All plots, unless noted, display the mean ± SD where *$p < 0.05$, **$p < 0.01$, and ***$p < 0.001$. See also Figure S1.

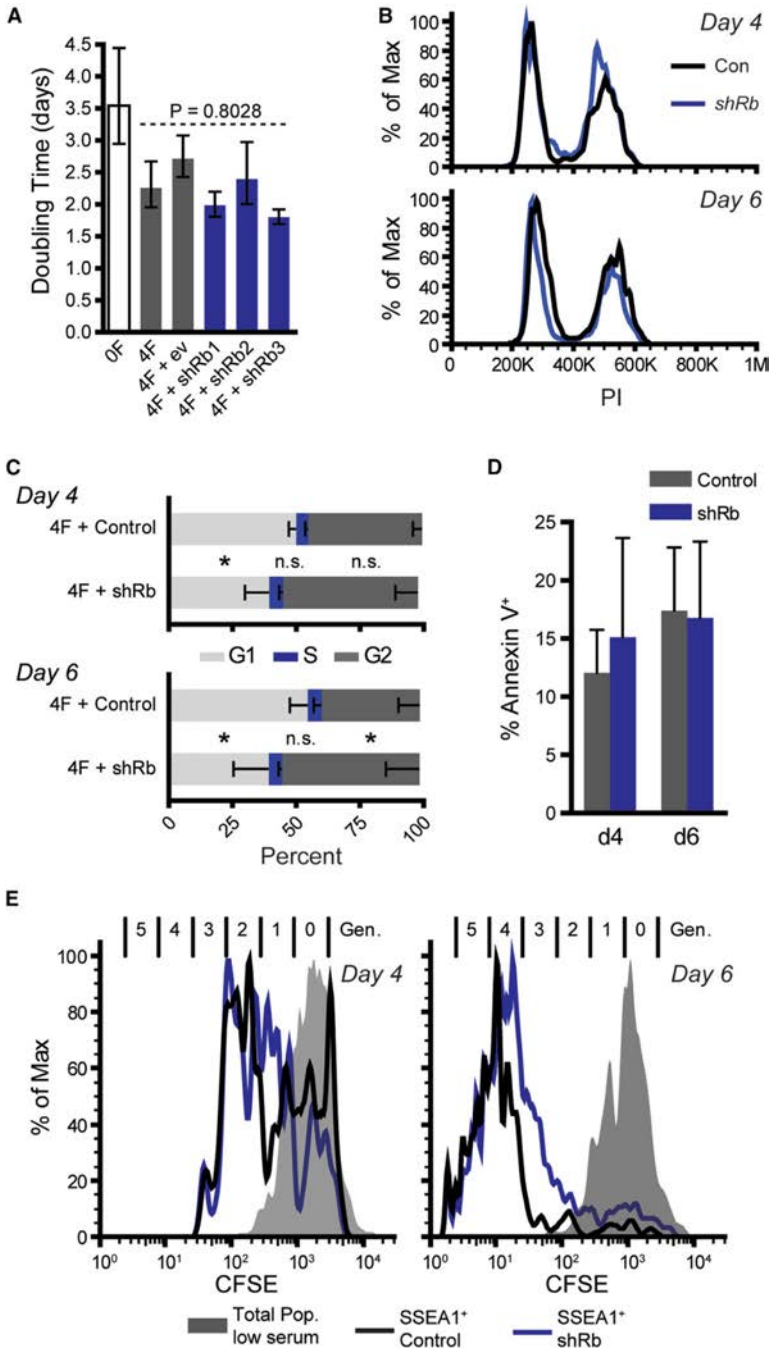

Figure 2. The Rb Block toward Reprogramming Is Not Cell Cycle Dependent

(A) Doubling time of shRb-infected *Oct4-GFP* MEFs after infection with 4F. Error bars reflect the 95% confidence interval and significance was assessed using ANOVA ($n \geq 3$).

(B) Cell cycle analysis on day 4 or day 6 by PI staining of shRb-infected *Oct4-GFP* MEFs infected with 4F on day 0. For clarity the 4F and 4F+ev controls were combined (Con), and the three hairpins were combined (shRb).

(C) Quantification of the cell cycle shown in (B). Significance was assessed by a t test ($n = 3$).

(D) Percent apoptosis as determined by Annexin V staining of *Oct4-GFP* MEFs either 4 or 6 days after 4F infection (n = 3).

(E) Number of generations (Gen) after 4F evaluated by CFSE staining of shRb-infected MEFs. MEFs were infected with 4F on day 0 and stained with CFSE on day 1. On days 4 or 6, the cells were stained with anti-SSEA1 and analyzed by FACS. The gray curve represents CFSE-stained MEFs grown in 0.5% serum to induce quiescence. The black and the blue curves represent the CFSE histogram for the $SSEA1^+$ control or shRb samples, respectively (n = 3).

All plots display the mean ±SD unless noted where $*p < 0.05$. See also Figure S2.

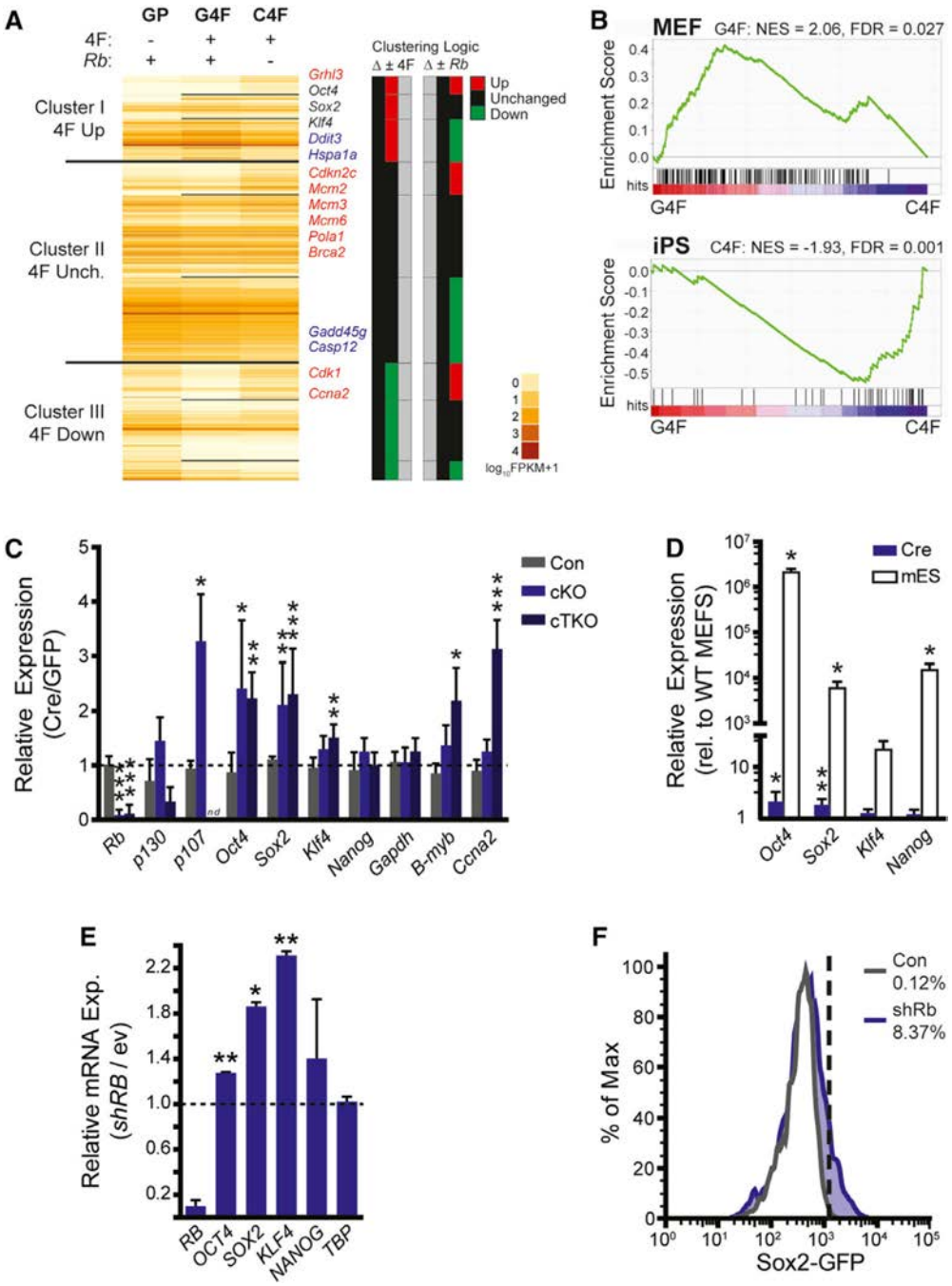

Figure 3. Rb Represses the Expression of Pluripotency Factors

(A) RNA sequencing of $Rb^{lox/lox}$ MEFs after *Rb* knockout by Cre expression (C) or GFP (G) followed by infection with an empty puromycin-selectable lentivirus (P) or the 4F. k-means clustering (Figures S3C and S3D) was first performed to divide the genetic expression levels that go up upon 4F expression (Cluster I), down (Cluster III), or remain unchanged (Cluster II) (G4F versus GP). Each of these clusters was then further divided by whether they change after loss of Rb (G4F versus C4F). Genes of interest are annotated on the left and are

marked red, blue, or black depending on whether their expression levels go up, down, or stay unchanged, respectively, in the C4F set (upon loss of Rb). See also Table S1.

(B) GSEA profiles comparing the G4F and C4F set to expression profiles of matched MEF and iPSCs (Table S1). The green graph shows the running enrichment score for the gene set as it is calculated running down the genes from the RNA sequencing (Figure 4A) that are ranked by their enrichment in either the G4F or C4F sets (red/ blue heatmap). Normalized enrichment scores (NESs) and false discovery rates (FDRs) for the gene sets are reported.

(C) Gene expression in control (Con, $Rb^{+/+}$; $p130^{+/lox}$; $p107^{+/+}$), cKO ($Rb^{lox/lox}$; $p130^{+/+}$; $p107^{+/+}$), and cTKO ($Rb^{lox/lox}$; $p130^{lox/lox}$; $p107^{-/-}$) MEFs as assessed by RT-qPCR. Expression is graphed as the relative expression of Ad-Cre-infected MEFs compared to that of Ad-GFP normalized to *Arppo*. Statistical significance was determined by a paired t test of the Ad-Cre and Ad-GFP ΔCt values. nd, no data.

(D) Expression measured by RT-qPCR for either *Rb* cKO MEFs infected with Ad-GFP or Ad-Cre (n = 4) or mESCs (n = 3), shown relative to the Ad-GFP cells. Statistical significance was determined by a paired t test of the Ad-Cre MEFs and an unpaired t test for the mESCs.

(E) Expression measured by RT-qPCR is graphed as the relative expression of shRB-infected human fibroblasts compared to those infected with an empty vector (ev) and normalized to *GAPDH*. Statistical significance was determined by a paired t test of the knockdown and control ΔCt values; n = 2.

(F) FACS analysis of GFP in *Sox2-GFP* knockin MEFs after shRb infection compared to controls. Dashed line demarcates GFP^+ gate.

All plots display the mean ± SD where *p < 0.05, **p < 0.01, and ***p < 0.001. See also Figure S3.

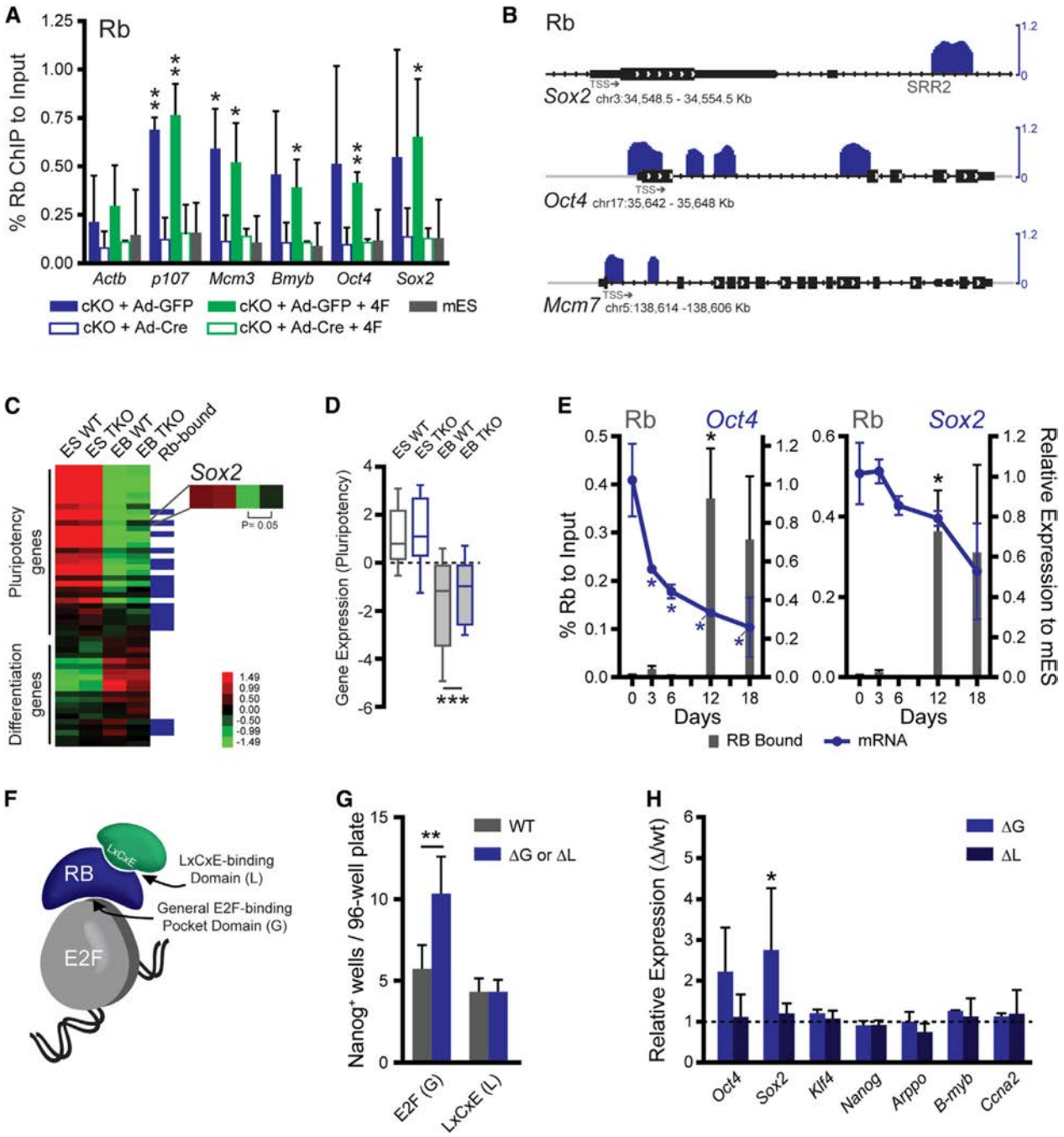

Figure 4. Rb Directly Binds Regulatory Elements in the *Oct4* and *Sox2* Loci

(A) qPCR of Rb ChIP in Ad-GFP-infected cKO MEFs compared to Ad-Cre-infected MEFs and the mESCs as negative control. Primers are to the proximal promoter (Table S4). Significance was assessed by an unpaired t test to the average of the Ad-Cre-infected MEFs, including the mESC sample (n = 2).

(B) Rb (blue) binding at *Sox2*, *Oct4*, and *Mcm7*. Enrichment is shown as the $\log_2$ value of the fold change between normalized ChIP and the input samples (n = 2). The transcription start sites (TSS) are noted.

(C) Gene expression by microarray of WT and TKO mESCs after their differentiation into embryoid bodies (n = 3). Pluripotency genes (Figure S4D) and a selection of differentiation markers from endoderm, mesoderm, ectoderm, and trophectoderm are shown. These are also scored for their status as direct Rb targets.
(D) The average expression of the pluripotency genes shown in (C). Plots show the mean (horizontal line), the 25^{th} to the 75^{th} percentile (box), and the extent of the data (bars). Significance was tested by a paired t test.
(E) Rb ChIP in mESCs (d0) and after their subsequent differentiation into EBs (d3, d6, d12, and d18). Binding is shown (gray bars, left axis) as percent input normalized to a control locus to further account for cell number. Expression from the locus (either *Oct4* or *Sox2*) is shown relative to the levels in the mESCs (blue line, right axis). Significance was determined by an unpaired t test to the respective d0 values for the ChIP and qPCR sets.
(F) Schematic of Rb interaction surfaces including the general E2F binding surface (G) and the LxCxE-binding domain (L), which interacts with other silencing factors.
(G) Reprogramming efficiency of the ΔG or ΔL mutant MEFs compared to those derived from a wild-type littermate. Efficiency was screened by AP and *Nanog* staining. Significance was determined by a paired t test.
(H) Gene expression in the ΔG and ΔL MEFs compared to wild-type MEFs as assessed by RT-qPCR. Expression is graphed as the relative expression of the mutant to the wild-type. Statistical significance was determined by a paired t test of the ΔCt values.
All plots, unless noted, display the mean ± SD where *$p < 0.05$, **$p < 0.01$, and ***$p < 0.001$. See also Figure S4.

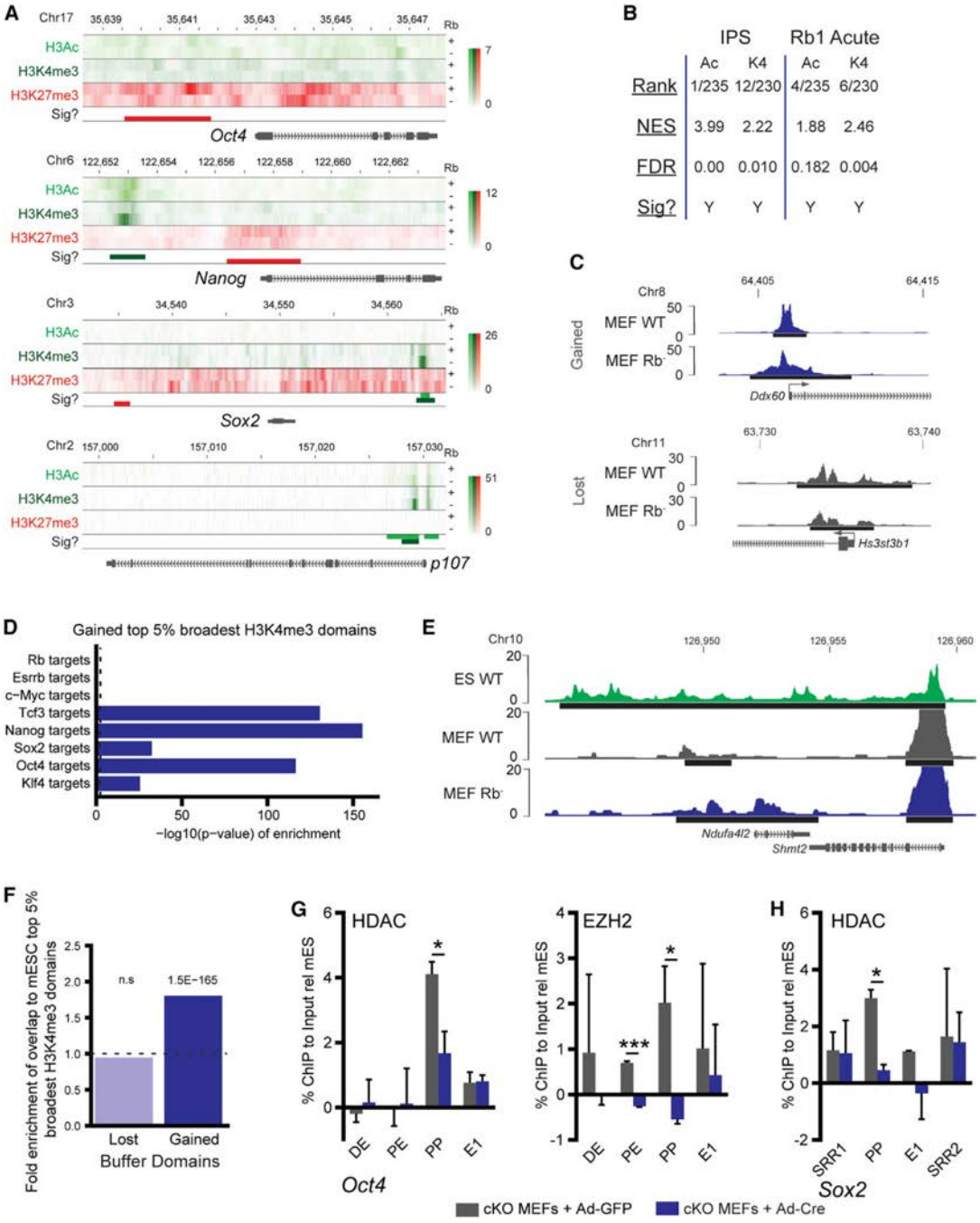

Figure 5. Rb Loss Perturbs the Chromatin State of Pluripotency Genes by Modulating Histone Modifier Recruitment

(A) Histone modification profiles for H3Ac (light green), H3K4me3 (dark green), and H3K27me3 (red) displayed as a heatmap. The bottom track indicates regions of significant changes for each mark by their respective color.

(B) GSEA results showing enrichment of iPSC and Rb gene sets upon gain of H3 acetylation and H3K4me3. Data shown are the rank of the gene set relative to all identified gene sets, the normalized enrichment score (NES), and the false discovery rate (FDR).

(C) Examples of genes that show an increase (blue) or decrease (gray) in H3K4me3 domain breadth upon loss of *Rb*. Black bars represent the extent of the domains.
(D) Significance for enrichment of transcription factor targets at genes that gained substantial H3K4me3 breadth in MEFs upon loss of Rb against the expected genome-wide value from 1,000 random samplings expressed as — log10 (p value) in one-sided Wilcoxon tests.
(E) Examples of a gene in which the H3K4me3 peak breadth in wild-type MEFs (gray) is broadened upon loss of Rb (blue), compared to mESCs (green). Horizontal black bars represent the extent of the peak.
(F) Fold-enrichment for overlap with top 5% broadest H3K4me3 domains ("buffer domains") for genes that lost or gained substantial H3K4me3 breadth in MEFs upon loss of Rb. Enrichment and significance (one-sided Wilcoxon tests) were calculated against expected genome-wide values from 1,000 random samplings.
(G) ChIP-qPCR of HDAC and EZH2 in Ad-GFP- and Ad-Cre-infected MEFs plotted relative to the mESCs as a negative control to account for relative primer strength. qPCR was performed with primers to the DE, PE, proximal promoter (PP), and first exon (E1) of *Oct4*. Significance was determined by a t test.
(H) ChIP-qPCR of HDAC binding shown as in Figure 5F, shown for the SRR1 and SRR2 enhancers, the PP, and the E1 of *Sox2*.
All plots, unless noted, display the mean ± SD where *$p < 0.05$ and ***$p < 0.001$. See also Figure S5.

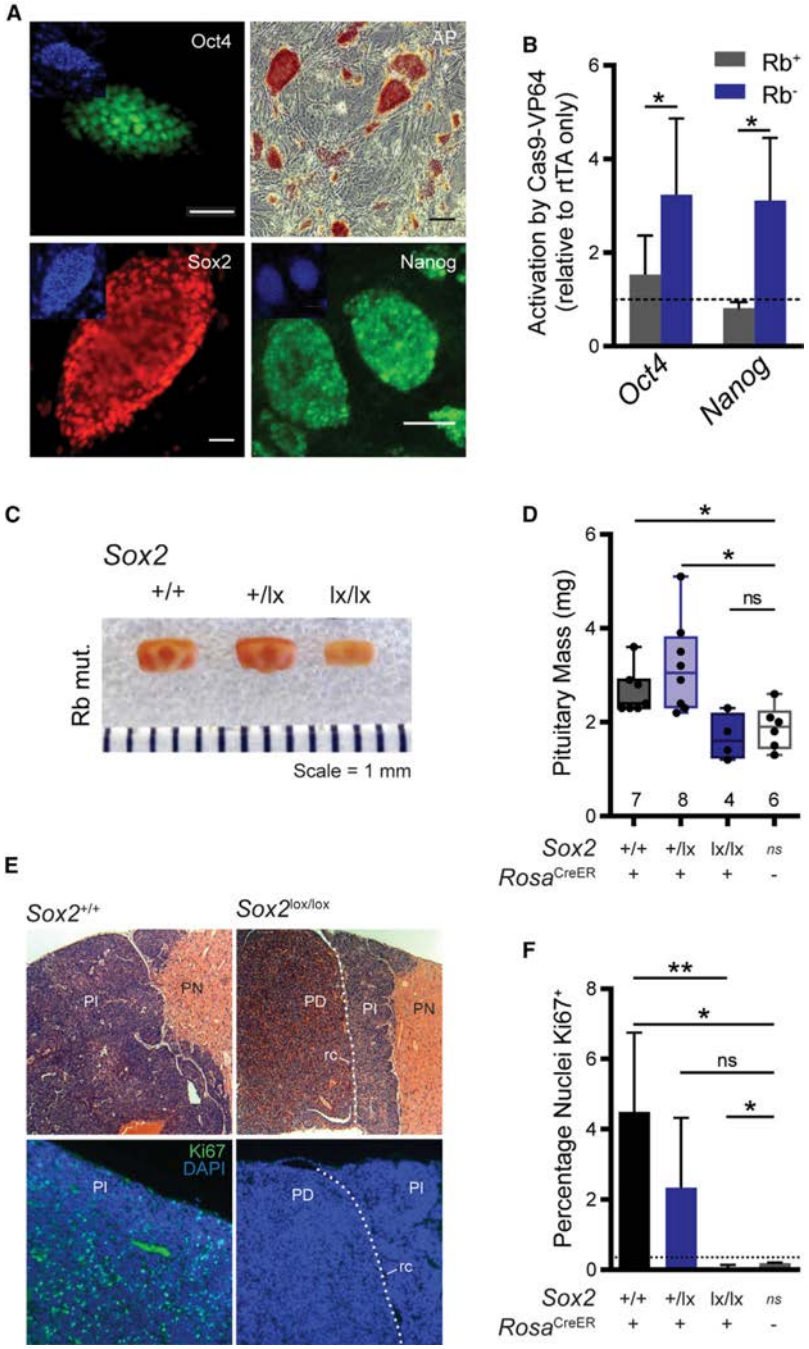

Figure 6. Rb Regulation of *Sox2* Affects the Need for Exogenous Factors to Generate iPSCs and Suppresses Phenotype in an Rb Tumor Model

(A) Staining of Rb^{KD} OKM iPSCs for *Oct4*, *Sox2*, *Nanog*, and AP activity. Scale bars, 100 mm, or 200 mm for AP.

(B) *Oct4* and *Nanog* were targeted for gene activation using the CRISPR-on technique (see Supplemental Experimental Procedures). RT-qPCR was performed 5 days after Cas9-VP64 activation and is shown relative to an rtTA-only control.

(C) Pituitaries from representative $Rb^{lox/lox}$; $Rosa26^{CreER}$ mice for all *Sox2* alleles (+, wild-type; lx, lox/lox) 9 weeks after tamoxifen injection.

(D) Box and whisker plots of the pituitary size from mice of the genotypes in Figure 6C, including *Rb*$^{lox/lox}$; *Rosa*$^{+/+}$ mice as controls.

(E) Pituitary sections of *Rb*$^{lox/lox}$; *Rosa26*^{CreER} mice that are either *Sox2*$^{+/+}$ or *Sox2*$^{lox/lox}$ 9 weeks after tamoxifen injection, stained with H&E (top) or Ki67 (bottom). The *Pars Nervosa* (PN), *Pars intermedia* (PI), *Pars distalis* (PD), and residual cleft (rc) are shown. The green channel was exposed equally between the two images. Representative images are shown.

(F) Quantification of Ki67 in *Rb*$^{lox/lox}$; *Rosa26*^{CreER} pituitaries with the shown *Sox2* genotypes (+, wild-type; lx, lox/lox) 9 weeks after tamoxifen injection. Percentages were calculated from four pituitaries, except the CreER^{-} control, which had n = 3. Dashed line indicates the number of positive cells counted in the secondary-only control.

All plots, unless noted, display the mean ± SD where *p < 0.05, **p < 0.01, and ns = not specified. See also Figure S6.